Pyczak, F.; Bauer, A.; Goeken, M.; Lorenz, U.; Neumeier, S.; Oehring, M.;
Paul, J.; Schell, N.; Schreyer, A.; Stark, A.; Symanzik, F.:

The effect of tungsten content on the properties of L12-hardened Co–Al–W alloys

In: Journal of Alloys and Compounds (2015) Elsevier

DOI: 10.1016/j.jallcom.2015.01.031

The effect of tungsten content on the properties of $L1_2$-hardened Co-Al-W alloys

Florian Pyczak[a*], Alexander Bauer[b], Mathias Göken[b], Uwe Lorenz[a], Steffen Neumeier[b], Michael Oehring[a], Jonathan Paul[a], Norbert Schell[a], Andreas Schreyer[a], Andreas Stark[a], Felix Symanzik[c]

[a]Institute of Materials Research, Helmholtz-Zentrum Geesthacht, Max-Planck-Strasse1, 21502 Geesthacht, Germany
[b] Friedrich-Alexander-Universität Erlangen-Nürnberg, Materials Science and Engineering, Institute I, Institute of General Materials Properties, Universität Erlangen-Nürnberg, Martensstrasse 5, 91058 Erlangen, Germany
[c]Institute of Materials Technology, Helmut-Schmidt-Universität, Holstenhofweg 85, 22043 Hamburg, Germany

[*]corresponding author: Florian Pyczak, Institute of Materials Research, Helmholtz-Zentrum Geesthacht, Max-Planck-Str. 1, D-21502 Geesthacht, Germany
E-mail: florian.pyczak@hzg.de
Telephone: +49 4152 87 2545

Abstract

Ternary Co-Al-W alloys with W contents between 8 and 11 at.% were investigated with respect to element partitioning, γ′ solvus, γ′ volume fraction, lattice mismatch and creep properties. W is enriched in the γ′ precipitates and an increasing W content stabilizes this phase. The lattice mismatch is positive up to 900 °C and rafting occurs during creep with a preferred direction in accordance with this positive lattice mismatch.

1. Introduction

While there is no stable $L1_2$-Co_3Al phase in the Co-Al binary system such a phase was recently found by Sato et al. [1] in the Co-Al-W system, which generated significant interest in this class of alloys. This is due to the fact that such alloys can benefit from the same precipitation hardening mechanisms as Ni-base superalloys. Recently doubts occurred whether this γ′-$L1_2$ phase in the Co-Al-W system is thermodynamically stable [2]. Even though transformations to other phases as reported in literature [2] take place after extended periods of time, these Co-base superalloys still have interesting prospects for alloy development.

For Ni-base superalloys it is well known that their mechanical properties strongly depend on the thermal stability, volume fraction and morphology of the γ′-$L1_2$ precipitation phase. The morphology and its change during high temperature deformation is itself influenced by the lattice mismatch between γ matrix and γ′ precipitates which depends on the partitioning behaviour of alloying elements between the matrix and the precipitate phase. Hence, these properties and especially γ′ solvus and volume fraction are also of interest for Co-base superalloys and a number of publications [3-10] investigate the possibilities to increase them by quaternary alloying additions. Some work [2,4,6,11-14], also often about quaternary alloys, covers the composition of single phases and/or partitioning behaviour of alloying elements. Unfortunately the information about lattice mismatch [1,4,10,15-17] and creep properties [7,9,15,17-20] are scarce by comparison until now. The present work investigates the partitioning behaviour, γ′ solvus temperature, γ′ volume fraction, lattice mismatch and creep properties for a set of ternary Co-Al-W alloys with systematically varied W content. From the phase diagram published by Sato et al. [1] it is clear that the Al content range of the γ/γ′ two-phase region is very narrow around 9 at.% but the W content stretches from below 8 at.% to above 11 at.%. So three experimental alloys are generated in this range of W contents to examine how variations in the W content influence the alloy properties. These results are then compared with selected literature data about quaternary alloying additions to judge how alloy properties can be influenced by only changing the W content in the ternary system.

2. Materials and Methods

Alloy ingots of about 90 g were produced in an arc melting unit with the nominal compositions Co-9Al-xW (x=8, 9, 11)-0.1B (concentrations are given in at.%). For the sake of brevity these alloys will be termed 8W, 9W and 11W in the following. The addition of boron should suppress grain boundary failure during compressive creep tests [21]. The actual composition of the three alloys was measured by energy dispersive X-ray (EDX) in the

scanning electron microscope (SEM). They were found to be Co-8.5Al-7.4W, Co-8.5Al-8.7W and Co-8.9Al-10.3W for 8W, 9W and 11W, respectively. For this an EDAX EDX system was used and the data was evaluated with the propriety EDAX software. Prior to the measurement the system was calibrated with a Co-Al-W standard. Due to the difficulty to quantitatively determine the boron content this element was excluded from the analysis. These specimens were solution heat treated at 1300 °C for 12 hours in a vacuum furnace. Subsequently, ageing treatments for up to 1000 hours at 900 °C in air were performed. While mainly results from the specimens aged for 200 hours are shown in the following it is noteworthy that also after 1000 hours of ageing no transformation or dissolution of the γ′ phase was observed. Also grain boundaries, which show a γ′ free seam and are decorated by borides, do not change their appearance during the annealing treatment up to 1000 h. The melting range and γ′ solvus temperature were measured in the as-cast state with a Netsch DSC 404 Pegasus system using a heating and cooling rate of 20 K/min. All data given about γ′ solvus, solidus and liquidus temperatures are from the heating part of the DSC curves. Specimens for microstructure characterisation were ground, polished and investigated in a Leo Gemini 1530 SEM with a field emission gun. The volume fraction of the γ′ phase was determined from the SEM micrographs using the line intersection method. For each alloy at least 150 precipitates per micrograph from two micrographs with image planes parallel to two different crystallographic {001} planes were evaluated. For TEM investigations specimens were cut and ground to about 100 μm thickness and subsequently electrolytically thinned to electron transparency using an agent of perchloric acid and butanol. The chemical composition of the phases γ and γ′ were measured by energy dispersive X-ray (EDX) using an Oxford INCA system at a Philips CM200 TEM operated at 200 kV in the STEM mode. The nominal spotsize was 2 nm and the TEM foil was oriented away from a two or multi beam diffraction condition to avoid channelling effects. Contrary to the SEM-EDX measurements described above the evaluation

of TEM-EDX results was performed standard-less using the propriety Oxford EDX software. TEM-EDX as applied in this work ~~on the other hand~~ was already used successfully for similar measurements in Ni-base superalloys [22, 23] with fine γ/γ′ microstructures. To describe the partitioning behaviour the partitioning coefficient $k_{\gamma'/\gamma}$ which is the concentration of an alloying element in the γ′ precipitate phase divided by the concentration in the γ matrix phase is used. The lattice constants were measured by high energy X-ray diffraction at the High Energy Materials Science (HEMS) beamline of the Helmholtz-Zentrum Geesthacht at the PETRA III storage ring of DESY in Hamburg, Germany, in transmission (photon energy of 87 keV / λ = 0.1425 Å). By fitting the respective sub-peaks to the overall shape of the (002) peak using Pseudo-Voigt functions the lattice constants of the phases γ and γ′ could be determined. Cylindrical specimens with a height of 7.5 mm and a diameter of 5 mm were creep deformed in compression up to about 3% plastic strain at 850 and 900 °C using stress levels of 460 and 275 MPa, respectively.

3. Results and Discussion

The microstructures of the alloys 8W, 9W and 11W after 200 h ageing at 900 °C are shown in figures 1 a), b) and c). All three alloys possess cubic γ′ precipitates but while the corners are slightly rounded in 8W and 9W, they are sharp in 11W. Also the width of γ channels decreases from 8W over 9W to 11W. During further annealing up to 1000 h the γ′ precipitates coarsen in all three alloys but their shape remains qualitatively the same (figures 1 d), e) and f)). More rounded particles are again found in 8W and 9W while the corners are sharp in 11W. No signs of a dissolution of the γ/γ′ microstructure or of transformation of the γ′ phase in other phases is observed. This finding does not necessarily mean that the γ′ phase is an equilibrium phase at 900 °C. Nevertheless, with respect to alloy development it can be stated that the γ′ phase is at least stable enough to be used as a hardening constituent for at least 1000 h at 900 °C in the range of alloy compositions investigated here.

Different transformation temperatures as γ′ solvus, and the solidus and liquidus temperatures of the alloys were evaluated from the respective peaks in the DSC curves. An example of the heating part of the DSC curve for the alloy 11W is shown in figure 2. Table 1 gives an overview about γ′ solvus, solidus and liquidus temperature as well as the volume fractions of the γ′ phase. With increasing W content the γ′ solvus temperature (onset) increases systematically by more than 50 K from 920 to 974 °C. The onset temperature giving the begin of γ′ dissolution should be less affected by the heating rate and be the most reliable data for γ′ solvus compared to peak and finish. On the contrary the liquidus and solidus temperatures vary only slightly by 7 to 10 K. This is in accordance with the binary Co-W phase diagram [6] which predicts no significant changes of the liquidus and solidus for variations of the W content in the range between 8 and 11 at.%. Also the γ′ volume fraction increases with increasing W content as also observed by Ooshima et al. [9]. While the relative increase of γ′ volume fraction and γ′ solvus with increasing W content is nearly equal for Ooshima's and this work, the absolute values reported by the former are higher for solvus temperature and in particular volume fraction. It can only be speculated whether this stems from different measurement parameters in both investigations as e.g. DSC heating rates.

3.1 Element partitioning γ/γ′

The chemical composition of the phases γ and γ′ which are given in table 2 are qualitatively in accordance with the ternary Co-Al-W phase diagram at 900 °C published by Sato et al. [1]. But it has to be mentioned that they are systematically higher than the overall composition of the three alloys measured by SEM-EDX. This is most probably due to the fact that SEM-EDX measurements where done with a system calibrated with a Co-Al-W standard while the evaluation of TEM-EDX results was done standard-less. Thus, with respect to absolute values the results of SEM-EDX are more reliable than TEM-EDX. While the Al content does not vary strongly between γ and γ′, W is significantly enriched in the γ′ phase, with the content

being higher by nearly 6 at.% in γ′ resembling the narrow Al and broad W range of the γ + γ′ two phase region. Nevertheless, the increase of the W content in the γ matrix by more than 2 at.% between 8W and 11W is not expected from the phase diagram [1,6]. It must be stated that in addition to systematic errors in TEM-EDX results due to the standard-less evaluation the W content variation in the γ phase is well in the range of the measurement errors. Especially, measurements in the specimen of 11W are difficult due to the rather narrow γ channels in this alloy. Thus, possible scientific explanations for this variation in the W content are only mentioned briefly here. It could either be, that the γ′ phase in the 11W alloy is metastable (i.e. not necessarily has to have a W content in accordance with the phase diagram published by Sato et al. [1]), that an equilibrium W distribution between γ and γ′ phase was not yet achieved due to the slower diffusion in 11W with its highest bulk W content, or that the γ+γ′ two phase field is broader than reported by Sato et al. [1]. The partitioning coefficients $k_{\gamma'/\gamma}$ of Co, Al and W in the alloys 8W, 9W and 11W are plotted in figure 3. It is clearly visible that neither Co nor Al partition strongly as both have partitioning coefficients near one. On the contrary, W is strongly enriched in the γ′ phase as evidenced by partitioning coefficients of 1.83±0.29 (8W), 1.65±0.16 (9W) and 1.58±0.34 (11W). In literature values in the range of 2 are reported for similar alloys [6,12] except for one paper by Meher et al. who found a significantly higher partitioning coefficient in the range of 6 [11]. Probably the fact that Meher investigated an alloy with lower Al and W content (about 5 at.% each) annealed at a lower temperature of 765 °C explains this difference. While the slight decrease of the partitioning coefficient with increasing W content between 8W, 9W and 11W in figure 3 is in the range of the measurement error, it is interesting to note that Shinagawa et al. found a similar behaviour for Ni-containing Co-base superalloys [4]. Hence, it cannot be fully dismissed that W tends to distribute more evenly between γ and γ′ phase for increasing W alloy content. Here, as in Shinagawa's paper, the decrease of the partitioning coefficient is

caused by an increase of the W content in the γ matrix phase which is not balanced by a similar increase in the γ′ precipitates.

By Omori et al. [13] partitioning coefficients for a large number of quaternary alloys were published. These are plotted as open symbols in figure 3. One can see that only Ti, Nb and Ta show a stronger partitioning behaviour than W. If this partitioning has the effect of stabilizing γ′ which manifests in an increased γ′ solvus temperature will be discussed in the following.

3.2 γ′ solvus

The γ′ solvus of the alloys 8W, 9W and 11W increases systematically by about 20 K per atomic percent W added to the alloy reaching 1036 °C in 11W. Similar increases of γ′ solvus with increased W content are found by Ishida [6] in quaternary Co-Al-W-Ni alloys. Also Titus et al. [18,20] and Omori et al. [13] report that the γ′ solvus of a ternary Co-Al-W alloy with W contents of 10 at.% or higher lies above 1000 °C. It is interesting to note, that Omori et al. [13] found a relationship between the enrichment of an element in the γ′ phase and an increase of the γ′ solvus temperature for a number of quaternary alloying elements. It is reasonable to assume that many alloying elements which enrich in the γ′ phase do so because it is energetically favorable and hence should also increase the γ′ solvus. Omori's data (open symbols) is shown in figure 4 together with the corresponding values for the ternary alloy 11W. The data for 11W lies only slightly above the linear fit to Omori's data and considering the measurement error of the partitioning coefficients agrees well with it. This means that the enrichment of W in the γ′ phase is connected with a stabilization of γ′ to higher temperatures and follows approximately the same relation as the other alloying elements. Nb, Ti and Ta, which partition stronger to the γ′ phase than W, also increase the γ′ solvus stronger. This is noteworthy with respect to alloy development because especially Ti and Nb have a lower density than W.

3.3 Lattice constants and lattice mismatch

Lattice constant data for the ternary Co-Al-W system was already published by Sato et al. [1]. Unfortunately since then the number of works about this topic remained rather limited [10,15-17]. This is especially true for elevated temperature data. One noteworthy result of all measurements published until now is the positive lattice mismatch. Here, as in most other works, the lattice mismatch is defined as $\delta = 2(a_{\gamma'}-a_{\gamma})/(a_{\gamma'}+a_{\gamma})$ with $a_{\gamma'}$ and a_{γ} being the lattice constants of the γ′ precipitate phase and γ matrix, respectively. These lattice constants of the phases γ and γ′ can be determined by fitting the overall (002) X-ray profile of the alloy with sub-peaks representing the contributions of the single phases to the overall peak. Examples for (002) X-ray profiles of the alloys 8W, 9W and 11W measured at room temperature are shown in figures 5 a, b and c. In figure 6 a) the lattice constants of the phases γ and γ′ for the alloys 8W, 9W and 11W are plotted. The lattice constant $a_{\gamma'}$ of the precipitate phase is always larger than that of the matrix phase a_{γ} and the lattice mismatch therefore positive in all three alloys. It is striking that a_{γ} increases continuously from 8W over 9W to 11W. The increase of the W content by more than 2 at.% in γ when comparing 8W with 11W is probably the reason for this. The lattice constants of the γ′ phase increase between 8W and 9W but are nearly equal for 9W and 11W. While the lattice constant of the γ matrix shows an almost linear dependence on the chemical composition of this phase as given in table 2 this is not the case for the γ′ phase. On the one hand that the change of the γ matrix lattice constant corresponds with the variation of the W content of the γ matrix in table 2 is a hint that despite the uncertainties of the TEM-EDX measurements, which were discussed earlier, these W content variations are really present. On the other hand there must be reasons why the lattice constant of the γ′ phase does not increase systematically with increasing W content. A possible reason is the very fine microstructure of alloy 11W with narrow γ matrix channels. What is measured here are constrained lattice constants because the interfaces between the γ and γ′ phase are coherent. Nevertheless, one would expect that the lattice constant of the γ phase in the narrow

matrix channels is more affected by the associated coherency stresses. Further mesasurements of lattice constants after long term annealing in 11W are necessary to answer this question. The intended service temperatures for these novel Co-base superalloys lie in the range between 500 and 1000 °C. Thus, the lattice mismatch at room temperature is only of minor interest for this material class as it can change significantly with temperature due to different thermal expansion of γ and γ′ and re-distribution of alloying elements between matrix and precipitates. Besides work from some of the present authors [15,17] only Tanaka et al. [16] and Yan et al. [10] published lattice mismatch data over temperature. This comprised data for a Ta and Ni containing alloy up to 900 °C [16] and for a Ti and a Ta containing alloy up to 750 °C [10]. In figure 6 b) the lattice mismatch as well as lattice constants of the phases γ and γ′ are plotted versus temperature. It has to be mentioned that this specimen is not identical with 9W but stems from another melt with the same nominal composition except that no boron is contained. With increasing temperature the lattice constants of γ as well as γ′ increase but to a larger extent for the γ matrix phase. This is especially pronounced above about 600 °C and a similar behavior is reported by Tanaka et al. [16]. Consequently, the lattice mismatch shows a pronounced decrease above 600 °C but remains positive with about 0.1 % at 900 °C. This is very different to Ni-base superalloys which either already possess a negative lattice mismatch at room temperature or change the sign of their lattice mismatch to negative when the temperature is increased [24]. On the opposite the Co-Al-W based alloys have a positive mismatch up to their γ′ solvus. From Tanaka's work one can see that this situation is also not changed by additions of alloying elements Ta and Ni to raise the γ′ solvus above 1000 °C.

3.4 Creep properties and morphology change

The compressive creep strength of the alloys 8W, 9W and 11W was tested at 850 °C and 900 °C applying stresses of 460 MPa and 275 MPa, respectively. The corresponding creep

curves are shown in figure 7. The creep curves of 9W and 11W show the typical shape with decreasing creep rate in the beginning, a stationary regime with a linear increase of plastic strain with creep time and accelerating creep in the end at 850 °C as well as at 900 °C. Due to the significantly faster creep of the alloy 8W the typical stages of the creep curve are neither discernible at 850 °C nor at 900 °C. The minimum creep rate is taken as a parameter to compare the three alloys with respect to creep strength. At 850 °C 11W has a minimum creep rate of 4.8×10^{-8} s^{-1} and 9W is only slightly worse with 5.2×10^{-8} s^{-1}. Only 8W with a minimum creep rate of 2.4×10^{-7} s^{-1} is significantly inferior. At 900 °C also the creep strength decreases from 11W over 9W to 8W with 2.7×10^{-8} s^{-1} (11W), 7.3×10^{-8} s^{-1} (9W) and 2.2×10^{-6} s^{-1} (8W). The difference between 11W and 9W is more pronounced at 900 °C which probably is due to the fact that, in addition to the solid solution hardening effects of W, the higher the creep temperature the more the difference in γ′ solvus temperature determines the relative creep strength of the alloys. Thus, the creep strength of the alloys increases at 850 °C as well as at 900 °C with increasing γ′ volume fraction, γ′ solvus temperature and W content. Compared with results from previous work of some of the authors [7,19] the results of a nominal Co-9Al-9W-0.1B alloy are worse than 9W but better than 8W. This discrepancy can probably be explained by slight variations in alloy composition. For creep tests at 900 °C data from Titus et al. exists for comparison [18,20]. There SX alloys with Ni and Ta additions were investigated which showed a better creep strength than 11W. It is noteworthy that also a ternary SX alloy with a composition rather similar to 11W exhibited a creep rate which was lower by one order of magnitude [18,20]. The difference in creep strength could stem from comparing different alloy compositions, polycrystalline and SX material or tensile and compressive creep tests.

The microstructures after creep deformation (figures 1g) h) i)) show pronounced rafting especially in 9W and 11W. The rafting direction perpendicular to the external compressive stress axis is caused by the positive mismatch at creep temperature and is different to Ni-base

superalloys which normally possess a negative lattice mismatch (e.g. as published by Pyczak et al. [24]). This is not an exclusive feature of the simple ternary alloys investigated here, as the more complex alloys investigated by Titus et al. [18] and Tanaka et al. [16] show also rafting behavior in accordance with a positive lattice mismatch. It is noteworthy that Mughrabi discussed in a recent work that such a positive lattice mismatch and the resulting change of the preferred rafting direction could be beneficial with respect to high temperature creep strength [25].

4. Conclusions

Variations of the W content in ternary Co-Al-W alloys alter the alloy properties in a comparable range as quaternary alloying element additions. For an increased W content the following effects on alloy properties were observed:

- W is enriched strongly in the γ′ phase but the partitioning to γ′ decreases with increasing W content.
- The γ′ solvus temperature and γ′ volume fraction increases with increasing W content.
- For W contents between 8 and 11 at.% the lattice mismatch is positive and remains so up to 900 °C
- During creep experiments in compression rafting perpendicular to the stress axis occurs due to the positive lattice mismatch.

So by increasing the W content it is possible to generate ternary alloys with reasonable creep strength compared to more complex Co-base superalloys. While theses alloys are not interesting from an alloy development point of view due to the high density of W compared to other alloying elements as for example Ti, these ternary Co-Al-W are a good system to investigate the fundamental microstructure property relationships in this class of Co-base superalloys.

Acknowledgements

The authors acknowledge the German Science Foundation (DFG) for funding project B3 of the collaborative research centre SFB/Transregio 103 and the DFG graduate school 1229.

References

[1] J. Sato, T. Omori, K. Oikawa, I. Ohnuma, R. Kainuma, K. Ishida, Cobalt-Base High-Temperature Alloys, Science 312 (2006**)** 90-91.

[2] S. Kobayashi, Y.Tsukamoto, T.Takasugi, H. Chinen, T. Omori, K. Ishida, S. Zaefferer, Determination of phase equilibria in the Co-rich Co–Al–W ternary system with a diffusion-couple technique, Intermetallics 17 (2009) 1085-1089.

[3] A. Suzuki, G. C. DeNolf, T.M. Pollock, Flow stress anomalies in c/c0 two-phase Co–Al–W-base alloys, Scripta Materialia 56 (2007**)** 385-388.

[4] K. Shinagawa, T. Omori, J. Sato, K. Oikawa, I. Ohnuma, R. Kainuma, K. Ishida, Phase equilibria and microstructure on γ′ phase in Co-Ni-Al-W system, Materials Transactions 49 (2008**)** 1474-1479.

[5] A. Suzuki, T.M. Pollock, High-temperature strength and deformation of γ/γ′ two-phase Co–Al–W-base alloys, Acta Materialia 56 (2008**)** 1288-1297.

[6] K. Ishida, Intermetallic Compounds in Co-Base Alloys-Phase Stability and Application to Superalloys, Mater. Res. Soc. Symp. Proc. 1128 (2009) 357-368.

[7] A. Bauer, S. Neumeier, F. Pyczak, M. Göken, Microstructure and creep strength of different γ/γ′-strengthened Co-base superalloy variants, Scripta Materialia 63 (2010) 1197-1200.

[8] T.M. Pollock, J. Dibbern, M. Tsunekane, J. Zhu, A. Suzuki, New Co-based γ-γ′ high temperature alloys, JOM 62 (2010) 58-63.

[9] M. Ooshima, K. Tanaka, N.L. Okamoto, K. Kishida, H. Inui, Effects of quaternary alloying elements on the γ′ solvus temperature of Co–Al–W based alloys with fcc/$L1_2$ two-phase microstructures, Journal of Alloys and Compounds 508 (2010) 71-78.

[10] H.-Y. Yan, V.A. Vorontsov, J. Coakley, N.G. Jones, H.J. Stone, D. Dye, Quaternary alloying effects and the prospects for a new generation of Co-base superalloys, Superalloys 2012 (Eds.: E.S. Huron, R.C. Reed, M.C. Hardy, M.J. Mills, R.E. Montero, P.D. Portella, J. Telesmann) TMS (2012) 705-714.

[11] S. Meher, H.-Y. Yan, S. Nag, D. Dyeb, R. Banerjee, Solute partitioning and site preference in γ/γ′ cobalt-base alloys, Scripta Materialia 67 (2012) 850-853.

[12] P.J. Bocchini, E.A. Lass, K.-W. Moon, M.E. Williams, C.E. Campbell, U.R. Kattner, D.C. Dunanda, D.N. Seidman, Atom-probe tomographic study of γ/γ′ interfaces and compositions in an aged Co–Al–W superalloy, Scripta Materialia 68 (2013) 563-566.

[13] T. Omori, K. Oikawa, J. Sato, I. Ohnuma, U.R. Kattner, R. Kainuma, K. Ishida, Partition behavior of alloying elements and phase transformation temperatures in Co-Al-W-base quaternary systems, Intermetallics 32 (2013) 274-283.

[14] I. Povstugar, P.-P. Choi, S. Neumeier, A. Bauer, C. H. Zenk, M. Göken, D. Raabe, Elemental partitioning and mechanical properties of Ti- and Ta-containing Co–Al–W-base superalloys studied by atom probe tomography and nanoindentation, Acta Materialia 78 (2014) 78–85.

[15] A. Bauer, S. Neumeier, F. Pyczak, M. Göken, Creep strength and microstructure of polycrystalline γ'-strengthened cobalt-base superalloys, Superalloys 2012 (Eds.: E.S. Huron, R.C. Reed, M.C. Hardy, M.J. Mills, R.E. Montero, P.D. Portella, J. Telesmann) TMS (2012) 695-703.

[16] K. Tanaka, M. Ooshima, N. Tsuno, A. Sato, H. Inui, Creep deformation of single crystals of new Co–Al–W-based alloys with fcc/$L1_2$ two-phase microstructures, Philosophical Magazine 92 (2012) 4011-4027.

[17] F. Pyczak, A. Bauer, M. Göken, S. Neumeier, U. Lorenz, M. Oehring, N. Schell, A. Schreyer, A. Stark, F. Symanzik, Plastic deformation mechanisms in a crept $L1_2$ hardened Co-base superalloy, Materials Science and Engineering A 571 (2013) 13-18.

[18] M.S. Titus, A. Suzuki, T.M. Pollock, Creep and directional coarsening in single crystals of new γ-γ′ cobalt-base alloys, Scripta Materialia 66 (2012) 574-577.

[19] A. Bauer, S. Neumeier, F. Pyczak, R.F. Singer, M. Göken, Creep properties of different γ′-strengthened Co-base superalloys, Materials Science and Engineering A 550 (2012) 333-341.

[20] M.S. Titus, A. Suzuki, T.M. Pollock, High Temperature Creep of New $L1_2$-containing Cobalt-base Superalloys, Superalloys 2012 (Eds.: E.S. Huron, R.C. Reed, M.C. Hardy, M.J. Mills, R.E. Montero, P.D. Portella, J. Telesmann) TMS (2012) 823-832.

[21] K. Shinagawa, T. Omori, K. Oikawa, R. Kainuma, K. Ishida, Ductility enhancement by boron addition in Co–Al–W high-temperature alloys, Scripta Materialia 61 (2009) 612-615.

[22] A. Volek, F. Pyczak, R.F. Singer, H. Mughrabi, Partitioning of Re between γ and γ′ phase in nickel-base superalloys, Scripta Materialia 52 (2005) 141-145.

[23] F. Pyczak, S. Neumeier, M. Göken, Temperature dependence of element partitioning in rhenium and ruthenium bearing nickel-base superalloys, Materials Science and Engineering A 527 (2010) 7939-7943.

[24] F. Pyczak, B. Devrient, H. Mughrabi, The effects of different alloying elements on the thermal expansion coefficients, lattice constants and misfit of nickel-based superalloys investigated by X-ray diffraction, Superalloys 2004 (Eds.: K.A. Green, T.M. Pollock, H. Harada, T.E. Howson, R.C. Reed, J.J. Schirra, S, Walston) TMS (2004) 827-836.

[25] H. Mughrabi, The importance of sign and magnitude of γ/γ′ lattice misfit in superalloys—with special reference to the new γ′-hardened cobalt-base superalloys, Acta Materialia 81 (2014) 21–29.

Table 1. Selected properties of the investigated alloys.

Alloy	γ´-solvus [°C] onset/ peak/ finish	Solidus [°C]	Liquidus [°C]	γ′ volume fraction [%]
8W	920/ 960/ 982	1457	1486	34
9W	927/ 985/ 1000	1459	1475	41
11W	974/ 1036/ 1049	1449	1479	73

Table 2. Chemical composition of the phases γ and γ' measured by TEM-EDX.

Alloy	c_γ [at.%]			$c_{\gamma'}$ [at.%]		
	Co	Al	W	Co	Al	W
8W	81.9 ±1.8	10.0 ±1.7	8.1 ±1.1	75.2 ±1.0	10.0 ±1.0	14.7 ±1.3
9W	81.7 ±0.7	9.3 ±0.4	9.0 ±0.7	75.7 ±1.5	9.5 ±0.7	14.8 ±0.8
11W	80.7 ±1.8	9.2 ±0.2	10.2 ±2.0	75.1 ±1.8	9.1 ±1.0	15.8 ±1,3

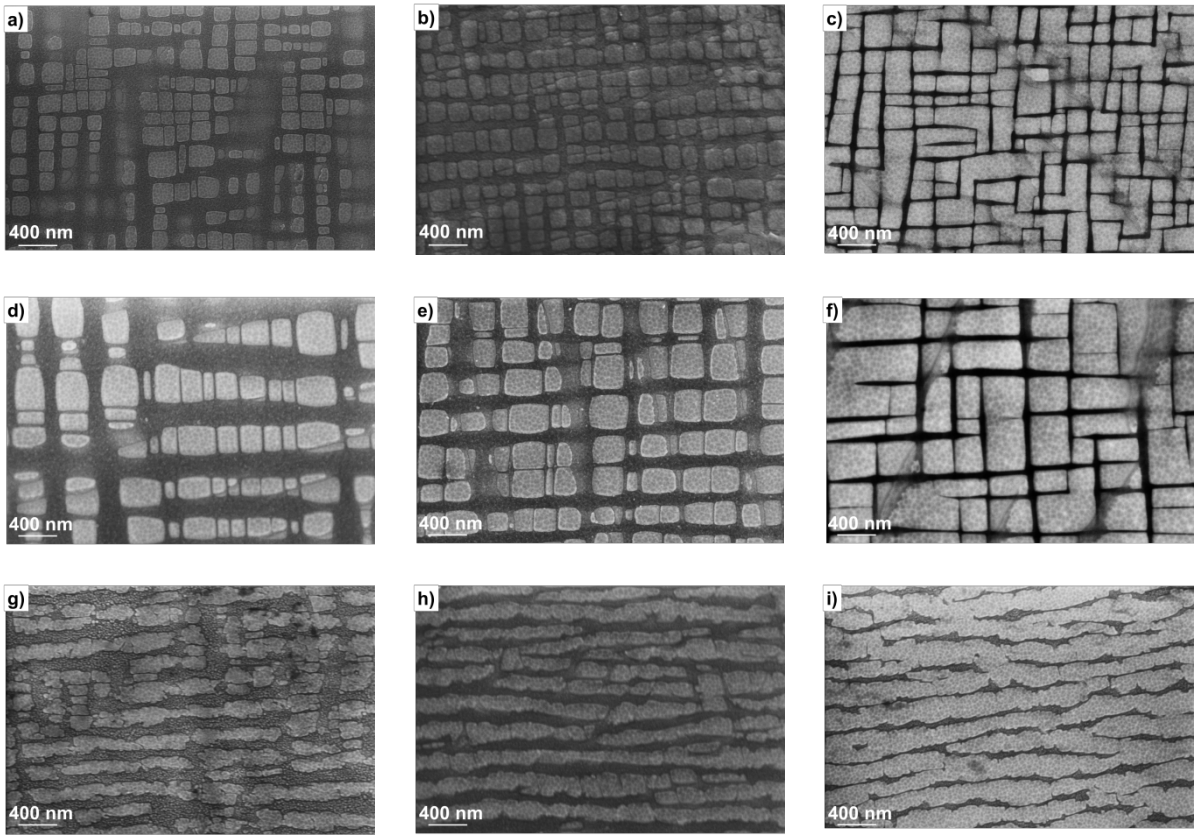

Fig. 1. Microstructure of the alloys investigated in this work; top: after solution heat treatment and ageing for 200h@900 °C – a) 8W b) 9W c) 11W;middle: after solution heat treatment and ageing for 1000h@900 °C – d) 8W e) 9W f) 11W; bottom: after creep with 275 MPa@900 °C (up to ca. 2 % plastic deformation) – g) 8W h) 9W i) 11W.

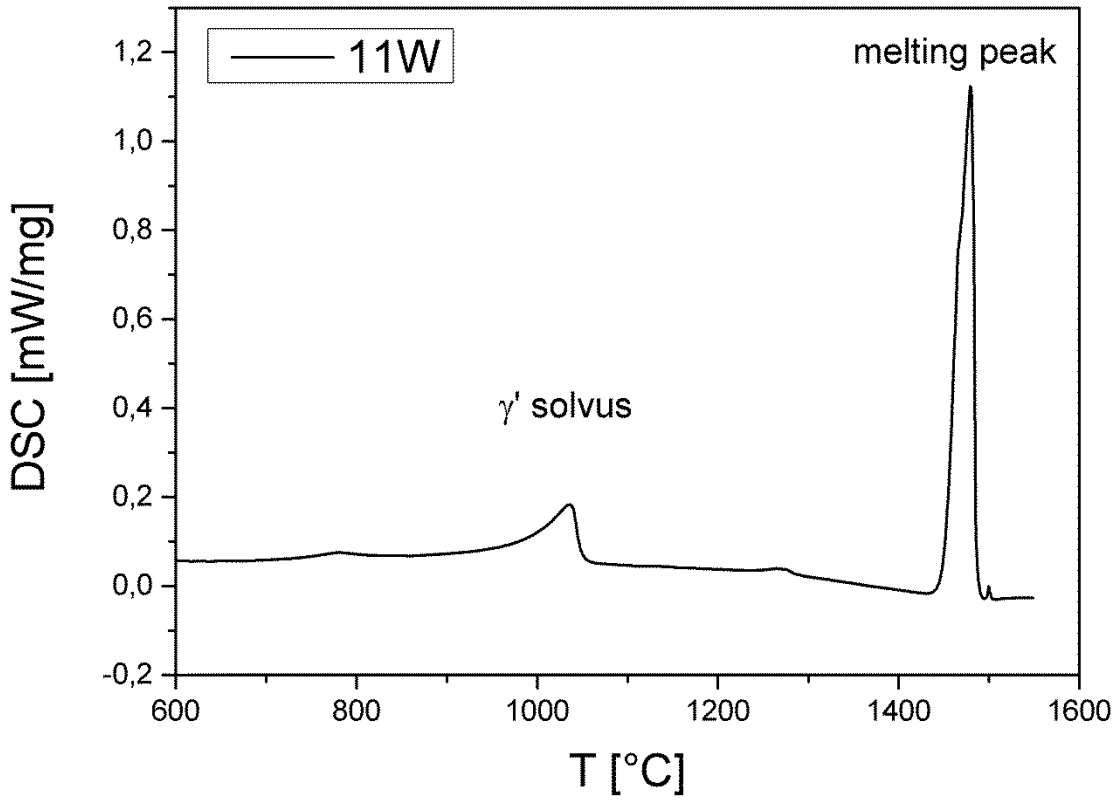

Fig. 2. DSC heating curve of the alloy 11W with the peaks of γ′ solvus and melting marked.

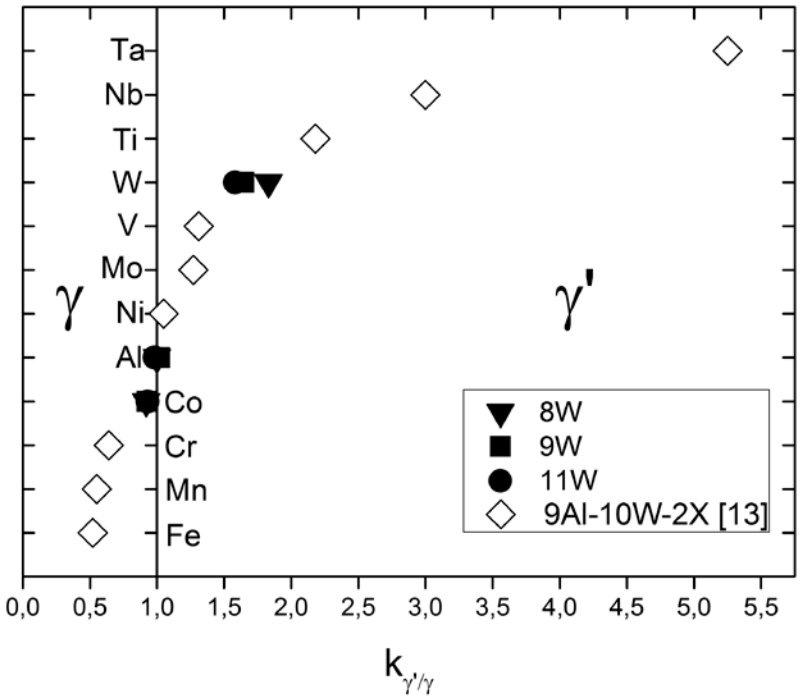

Fig. 3. Partitioning coefficients measured in this work (full symbols) plotted together with results by Omori et al. [13] for quaternary alloying additions (open symbols).

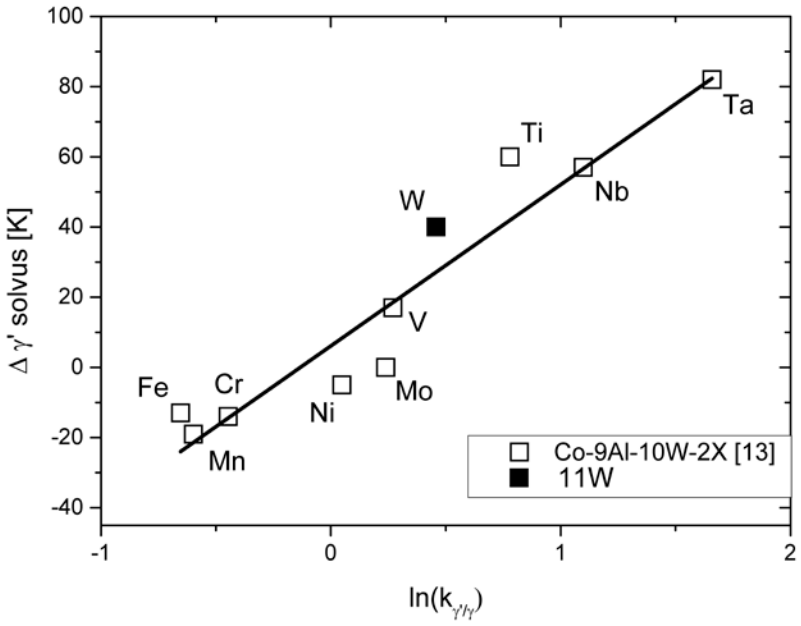

Fig. 4. Increase of γ′ solvus for 2 at.% addition of an alloying element plotted vs. partitioning coefficients; full symbol is for alloy 11W in this work and open symbols from data by Omori et al. [13].

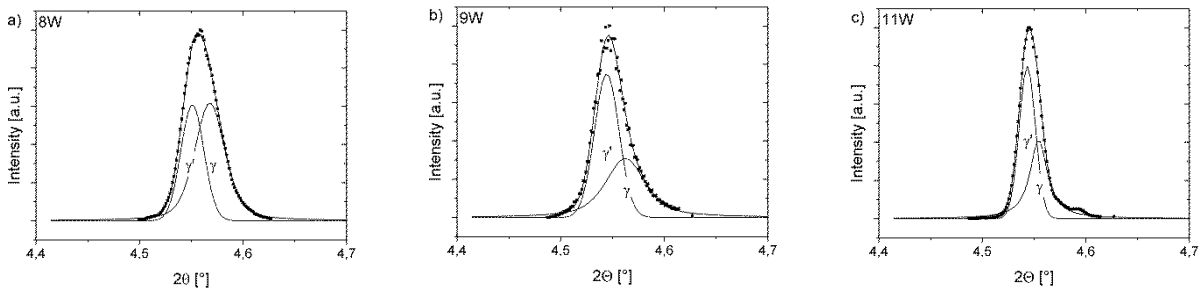

Fig. 5. (002) X-ray diffraction peaks of the alloys a) 8W, b) 9W and c) 11W; the Pseudo-Voigt peaks used to fit the contribution of the γ and γ' phase to the overall peak as well as the sum of the fitted sub-peaks are drawn as lines while the measured data is represented as points.

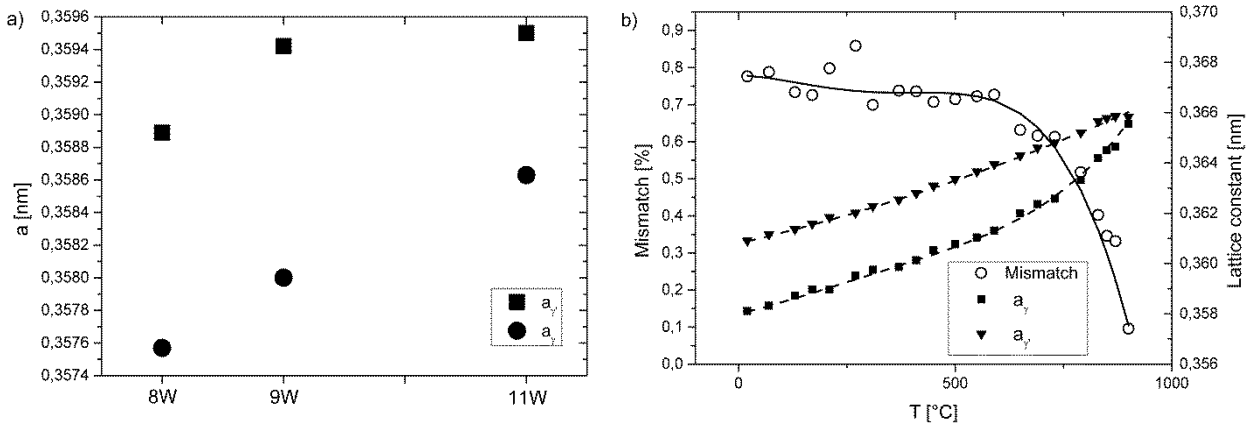

Fig. 6. a) Lattice constants of the phases γ and γ′ at room temperature for alloys 8W, 9W and 11W; b) temperature dependence of lattice constants of phases γ and γ′, and lattice mismatch for Co-9Al-9W.

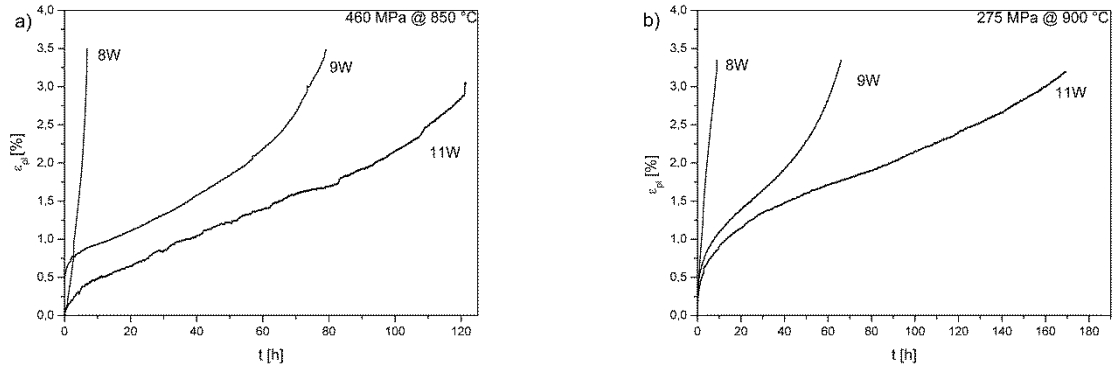

Fig. 7. Creep curves (plastic strain versus time) for the alloys 8W, 9W and 11W tested at a) 850 °C under 460 MPa load and b) 900 °C under 275 MPa load.